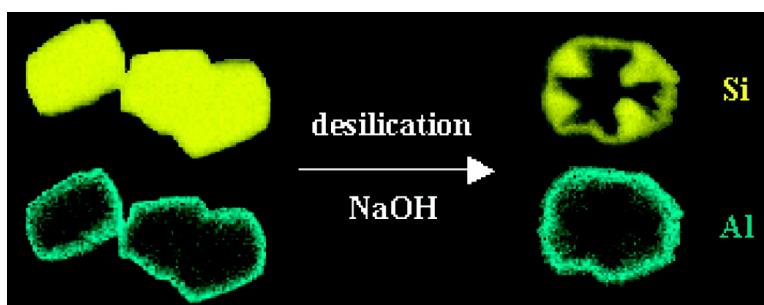## Communication

Creation of Hollow Zeolite Architectures by Controlled Desilication of Al-Zoned ZSM-5 Crystals

Johan C. Groen, Torkel Bach, Ulrike Ziese, Anne M. Paulaime-van Donk, Krijn P. de Jong, Jacob A. Moulijn, and Javier Prez-Ramrez

More About This Article

Additional resources and features associated with this article are available within the HTML version:

- Supporting Information
- Links to the 8 articles that cite this article, as of the time of this article download
- Access to high resolution figures
- Links to articles and content related to this article
- Copyright permission to reproduce figures and/or text from this article

View the Full Text HTML

Creation of Hollow Zeolite Architectures by Controlled Desilication of Al-Zoned ZSM-5 Crystals

Johan C. Groen,*,† Torkel Bach,‡ Ulrike Ziese,§ Anne M. Paulaime-van Donk,† Krijn P. de Jong,§ Jacob A. Moulijn,† and Javier Pérez-Ramírez∥

DelftChemTech, Delft University of Technology, Julianalaan 136, 2628 BL Delft, The Netherlands, Hydro Corporate Research Centre, P.O. Box 2560, N-3908, Porsgrunn, Norway, Inorganic Chemistry and Catalysis, Debye Institute, Utrecht University, Sorbonnelaan 16, 3584 CA Utrecht, The Netherlands, and Catalan Institution for Research and Advanced Studies (ICREA) and Institute of Chemical Research of Catalonia (ICIQ), Av. Països Catalans 16, E-43007, Tarragona, Spain

Received April 21, 2005; E-mail: j.c.groen@tnw.tudelft.nl

Zeolites are crystalline aluminosilicates that possess an exceptional combination of properties such as high thermal stability, Brønsted acidity, and microporosity. Accordingly, these materials are frequently practiced in industrial processes, for example, fluid catalytic cracking (Y), cumene production (mordenite), and toluene disproportionation and xylene isomerization (ZSM-5).

The presence of regular micropores of molecular dimensions is responsible for the zeolites' unequaled shape selectivity in catalytic conversions and separations, but this feature also poses diffusional limitations due to the restricted transport of molecules to and from the active sites. As a consequence, generation of mesoporosity in microporous crystals is attracting significant research interest.[1,2] The created mesopores facilitate physical transport and should lead to a more effective use of these materials. Desilication, that is, extraction of framework Si, is an efficient methodology to create intracrystalline mesoporosity in MFI-type zeolites.[3,4] The Si extraction and related mesopore formation is controlled by framework Al, and an optimal bulk Si/Al ratio of 25−50 has been identified.[5] A high framework Al concentration prevents Si extraction, while a low Al concentration leads to excessive extraction and formation of large pores. However, how the porosity is distributed throughout the crystals and the effect of crystal size is practically ignored. This information is indispensable to rationally devise potential applications of alkaline-treated zeolites.

The occurrence of Al zoning, that is, an Al-rich external surface as compared to the bulk aluminum concentration, is well-known in large ZSM-5 crystals.[6,7] Accordingly, it can be anticipated that this Al gradient will affect the Si extraction throughout the zeolite particle. Dessau et al.[8] have observed the nonuniform dissolution of large ZSM-5 crystals (5−10 μm) upon prolonged treatment at high concentrations of alkaline solution. This was speculatively attributed to the nonuniform concentration of Al in the crystals. However, a systematic study on the impact of Al gradients and the effect of crystal size to tailor the porosity development under optimized treatment conditions has not yet been accomplished.

Here we show that by controlled desilication of both large and small ZSM-5 crystals we have been able to address and make use of the impact of Al-zoning on the mesoporosity development. The presented approach provides a thus-far unused method to tailor the fabrication of hollow zeolite crystals, offering clear advantages to other methodologies pursuing hollow zeolite entities.[9,10] Our results are of fundamental interest in materials science and may open auspicious uses of alkaline-treated zoned ZSM-5 zeolites.

Two procedures were applied to synthesize ZSM-5 zeolite with small (SZ) and large (LZ) crystals in the optimal bulk Si/Al range of 25−50. The alkaline treatment was performed as described in the Supporting Information. The chemical composition and textural properties of the nontreated (nt) and alkaline-treated (at) zeolites are listed in Supporting Information Table S1.

The large crystals show a twinned character and are ca. 20 μm (Figure 1a). The Langmuir-type isotherm as obtained by N_2 adsorption on the nontreated sample confirms a minor mesoporosity contribution (Figure 1b). The presence of a marked Al gradient in the nontreated crystals is clearly evidenced by SEM-EDX displaying a more intense blue color at the external surface (Figure 1c). Point analysis on multiple crystals has revealed that the aluminum concentration at the outer surface is up to 30 times higher than that in the center of the crystals, while silicon and oxygen were rather homogeneously distributed (Figure S1). Alkaline treatment of these large crystals leads to only limited extra mesoporosity, as can be concluded from N_2 adsorption (Figure 1b and Table S1), while Hg porosimetry points to the formation of large voids in the range 1−5 μm with a significant macropore volume (Table S1). SEM-EDX on alkaline-treated crystals reveals an internal porosity development in the micrometer-size range, associated with the low concentration of Al in the interior of the crystals (Figure 1d,e). The preferential directions of the porosity development likely originate from the twinned nature of the crystals and different crystal interfaces.[11] The outer surface of the crystals remains relatively intact, which is attributed to the high concentration of Al in this region, confirming its crucial suppressing role in the Si extraction.[5]

The size of SZ crystals generally ranges from 400 to 700 nm (Figure 2a). The N_2 adsorption isotherm of SZ-at30 (30 min alkaline treatment) in Figure 2b exhibits an enhanced uptake and a distinct hysteresis loop, indicative of substantial mesoporosity development. The mesopore surface area increases from 25 to 180 m^2 g^{-1}. In contrast to the 2D-TEM micrographs of the nontreated sample that show hardly any contrast differences within the crystal, pointing to a uniform "solid" particle (Figure 2c), the micrographs of the alkaline-treated sample (Figure 2d) reveal significant mesoporosity. A dark rim of material, however, encloses the highly porous alkaline-treated crystals. The application of an advanced 3D-TEM[12] technique enables additional spatial resolution of the mesoporosity distribution throughout the small zeolite crystals. A virtual cross section through the reconstruction of a ca. 400-nm crystal shows a rather uniform mesoporosity development in the interior of the crystal (Figure 2e), while the outer surface remains relatively unaffected. A surface rendering clearly shows a shell of zeolite material encapsulating the porous interior (Figure 2f). Although the H1 hysteresis loop in the isotherm of SZ-at30 does not conclu-

---

† Delft University of Technology.
‡ HydroCorporate Research Centre.
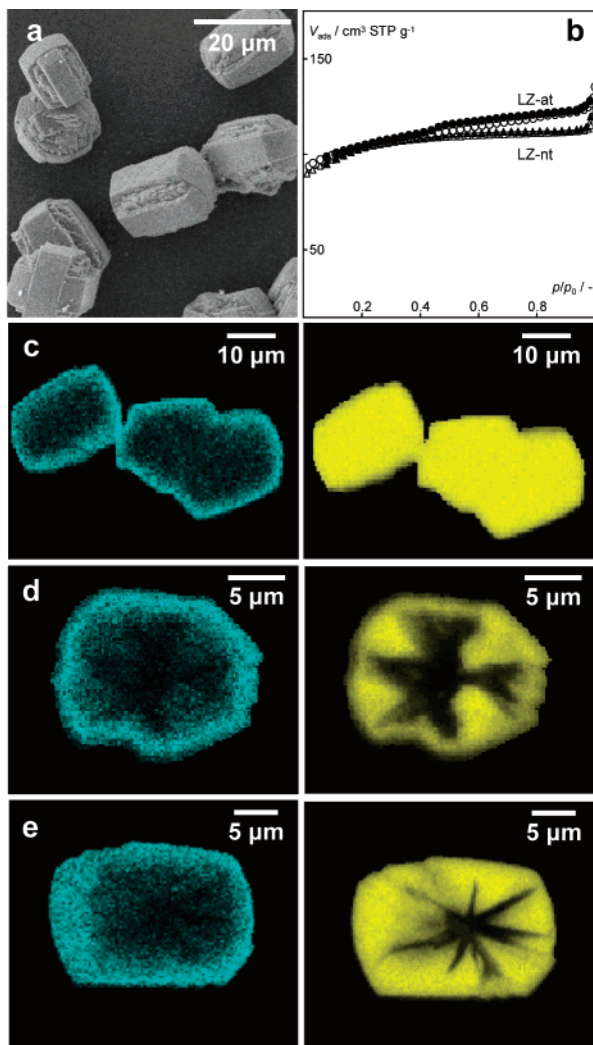§ Utrecht University.
∥ ICREA and ICIQ.

Figure 1. (a) SEM micrographs of LZ-nt. (b) N$_2$ adsorption isotherms at 77 K of LZ-nt and LZ-at. (c,d) SEM-EDX images of polished nontreated (c) and alkaline-treated (d,e) crystals. Blue and yellow colors represent aluminum and silicon, respectively.

sively indicate any enclosed porosity, application of a shorter treatment time of 15 min (SZ-at15) results in a pronounced H2 hysteresis loop with a forced closure at $p/p_0 = 0.42$ (Figure 2b). H2-type hysteresis is a result of the presence of voids or cavities that can only be accessed via entrances smaller than 4 nm, indeed pointing toward a relatively intact outer surface. This proves that the accessibility to the internal mesoporosity can be furthermore tuned by optimization of the treatment parameters. The variation in internal porosity development in the small and large crystals must be attributed to differences in the Al gradient and connected local Si extraction. As the spatial distribution of aluminum can be controlled in the synthesis,[13] an optimal tailoring of the final porous properties upon desilication of both small and large zeolite crystals can be envisaged.

We have shown that, when subjected to controlled desilication conditions, Al gradients in both large and small ZSM-5 crystals induce the formation of hollow particles with a well-preserved Al-rich exterior, further confirming the crucial role of Al in the mechanism of Si extraction.[5] Desilication coupled to 3D-TEM reveals to be a suitable tool to elucidate aluminum gradients in small zeolite crystals. Our methodology enables the fabrication of highly porous hollow particles on various length scales with tunable void volumes and sizes and accessibility. Particularly the high degree of mesoporosity offers perspectives as hosts for enclosure
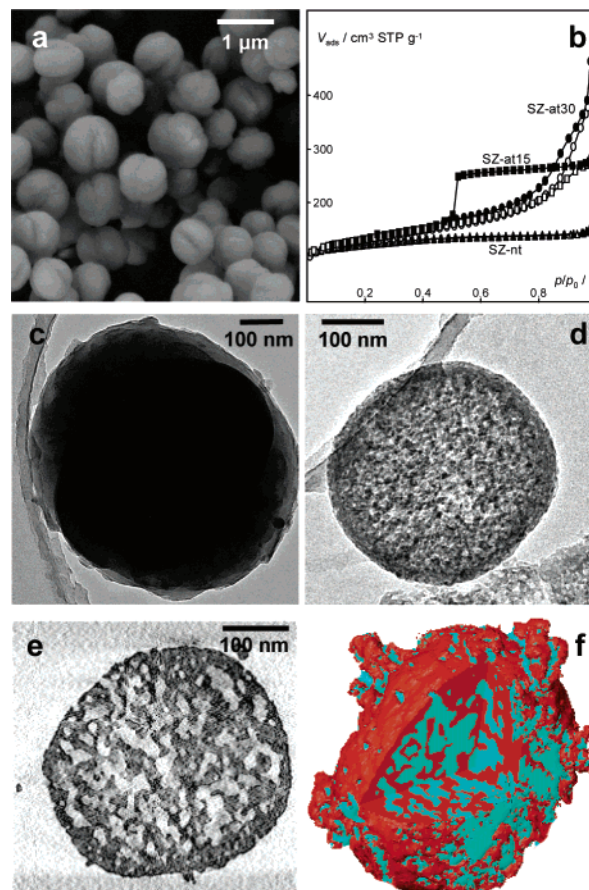

Figure 2. (a) SEM micrograph of nontreated SZ-5 crystals. (b) N$_2$ adsorption isotherms at 77 K of SZ-nt and SZ-at. (c) TEM micrograph of SZ-nt. (d) TEM micrograph of SZ-at. (e) 3D-TEM virtual cross sections through the reconstruction of an alkaline-treated 400-nm crystal. (f) Surface rendering of alkaline-treated 400-nm crystal; zeolite material orange, porosity blue. A section was cut out to obtain an inside view of the particle.

of chemical entities (e.g., nanoparticles),[14] while in this case having a functional microporous barrier.

Supporting Information Available: Synthesis and alkaline treatment procedures, textural properties, and results of SEM-EDX point analysis. This material is available free of charge via the Internet at http://pubs.acs.org.

References

(1) Van Donk, S.; Janssen, A. H.; Bitter, J. H.; de Jong, K. P. *Catal. Rev.* **2003**, *45*, 297−319.
(2) Jacobsen, C. J. H.; Madsen, C.; Houzvicka, J.; Schmidt, I.; Carlsson, A. *J. Am. Chem. Soc.* **2000**, *122*, 7116−7117.
(3) Ogura, M.; Shinomiya, S.; Tateno, J.; Nara, Y.; Kikuchi, E.; Matsukata, M. *Chem. Lett.* **2000**, 882−883.
(4) Groen, J. C.; Peffer, L. A. A.; Moulijn, J. A.; Pérez-Ramírez, J. *Colloid Surf., A* **2004**, *241*, 53−58.
(5) Groen, J. C.; Jansen, J. C.; Moulijn, J. A.; Pérez-Ramírez, J. *J. Phys. Chem. B* **2004**, *108*, 13062−13065.
(6) Derouane, E. G.; Detremmerie, S.; Gabelica, Z.; Blom, N. *Appl. Catal.* **1981**, *1*, 201−224.
(7) von Ballmoos, R.; Meier, W. M. *Nature* **1981**, *289*, 782−783.
(8) Dessau, R. M.; Valyocsik, E. W.; Goeke, N. H. *Zeolites* **1992**, *12*, 776−779.
(9) Wang, X. D.; Yang, W. L.; Tang, Y.; Wang, Y. J.; Fu, S. K.; Gao, Z. *Chem. Commun.* **2000**, 2161−2162.
(10) Dong, A.; Ren, N.; Yang, W.; Wang, Y.; Zhang, Y.; Wang, D.; Hu, J.; Gao, Z.; Tang, Y. *Adv. Funct. Mater.* **2003**, *13*, 943−948.
(11) Geus, E. R.; Jansen, J. C.; van Bekkum, H. *Zeolites* **1994**, *14*, 82−88.
(12) Janssen, A. H.; Koster, A. J.; de Jong, K. P. *Angew. Chem., Int. Ed.* **2001**, *40*, 1102−1104.
(13) Althoff, R.; Schulz-Dobrick, B.; Schüth, F.; Unger, K. *Zeolites* **1993**, *1*, 207−218.
(14) Christensen, C. H.; Schmidt, I.; Carlsson, A.; Johanssen, K.; Herbst, K. *J. Am. Chem. Soc.* **2005**, *127*, 8098−8102.

JA052592X